

are actually characteristic of shorter radii than those at which they are plotted in Fig. 3, and the predicted flattening is thus concealed.

# VII. CONCLUSION

Although the methods of calculation used in this work could be considerably refined, for instance, in allowing for the effects of diffraction and orbit perturbation by neutron capture, it seems better to await further data which confirm the rather surprisingly large size of the  $\text{Be}^9$  nucleus indicated here. As the study of heavy ion interactions proceeds, neutron pickup may be found from beryllium using even heavier projectiles and under circumstances where the orbital picture is less blurred than in the present case.

The idea of using such a classical approach for the interpretation of heavy ion nuclear collisions is not new. It has been developed in a series of papers by Breit and his collaborators,<sup>11</sup> and has been applied to the reaction  $\text{Au}^{197}(\text{N}^{14}, \text{N}^{13})\text{Au}^{198}$  by McIntyre, Watts, and Jobes.<sup>12</sup>

# ACKNOWLEDGMENTS

My thanks are due to E. Norbeck, Jr., for sending a preprint of the experimental work of Norbeck, Blair, Pinsonneault, and Gerbracht. I am also indebted to Professor G. Wentzel for discussions and suggestions.

<sup>11</sup> G. Breit, M. H. Hull, and R. L. Gluckstern, *Phys. Rev.* **87**, 74 (1952) and following papers.

<sup>12</sup> J. A. McIntyre, T. L. Watts, and F. C. Jobes, *Phys. Rev.* **119**, 1331 (1960).

# Elastic Scattering of Fast Neutrons by Tritium and $\text{He}^3$

J. D. SEAGRAVE, L. CRANBERG, AND J. E. SIMMONS

*Los Alamos Scientific Laboratory, University of California, Los Alamos, New Mexico*

(Received May 9, 1960)

Differential cross sections have been obtained for the elastic scattering of neutrons by tritium and by  $\text{He}^3$  at  $E_n = 1.0, 2.0, 3.5$ , and  $6.0$  Mev over the angular range  $27^\circ$  to  $161^\circ$  in the c.m. system. The Los Alamos large Van de Graaff accelerator and pulsed-beam time-of-flight facility were employed, and the scattering samples were contained in small thin-walled stainless steel spheres. One-third mole of  $\text{He}^3$  was contained at 5000 psi and one-half mole of tritium was prepared in the form of  $\text{CaT}_2$ . Absolute cross sections were determined from a comparison with the scattering from a thin shell of  $\text{CH}_2$  at each energy, together with calibration of the relative sensitivity of the detector as a function of energy by the known forward yield of the  $\text{T}(p, n)\text{He}^3$  reaction. The angular distributions for  $n$ -T scattering are in excellent agreement with the calculations of Bransden, Robertson, and Swan based on a Serber exchange force. The  $n$ - $\text{He}^3$  measurements favor qualitatively the Serber rather than the symmetrical exchange force used in the calculations, but the agreement is poorer than that obtained for  $n$ -T scattering. The polarization of elastically scattered 1-Mev neutrons was found to be less than 5% for both samples, unlike the strong polarization observed in  $n$ - $\text{He}^4$  scattering.

# INTRODUCTION

THE measurements reported in this paper are concerned with the elastic scattering of fast neutrons by nuclei of mass three. They are part of an extensive program of investigation at this Laboratory of the interactions of the very light nuclei. The long-range objective of this program is to reconcile the scattering, reaction, and ground-state properties of the very light nuclei with the information about nuclear forces derived from analysis of  $n$ - $p$  and  $p$ - $p$  scattering. Supplementary knowledge of nuclear forces may be sought in the study of excited states and interactions in systems of a few nucleons. From the latter point of view, neutron scattering by the very light nuclei is of special interest since direct observation of the scattering of neutrons is not feasible at present, and the character of the  $n$ - $n$  force must be inferred from a study of the interactions

of neutrons with bound systems of nucleons. The possibility of many-body nuclear forces can also be investigated through the study of systems of a few nucleons.

Much theoretical and experimental effort has been devoted to the study of  $p$ - $d$  and  $n$ - $d$  interactions. Reviews of the subject have been given by Massey<sup>1</sup> and by Mather and Swan.<sup>2</sup> A bibliography of more recent experimental work will be found in recent papers on  $n$ - $d$  elastic and  $p$ - $d$  inelastic scattering.<sup>3,4</sup> The calculation of nucleon-deuteron interactions with tensor forces has been formulated,<sup>5</sup> but the present state of nucleon-deuteron scattering theory is inconclusive.

<sup>1</sup> H. S. W. Massey, *Progress in Nuclear Physics*, edited by O. R. Frisch (Pergamon Press, New York, 1953), Vol. 3, pp. 235-270.

<sup>2</sup> K. B. Mather and P. Swan, *Nuclear Scattering* (Cambridge University Press, New York, 1958).

<sup>3</sup> J. D. Seagrave and L. Cranberg, *Phys. Rev.* **105**, 1816 (1957).

<sup>4</sup> L. Cranberg and R. K. Smith, *Phys. Rev.* **113**, 587 (1959).

<sup>5</sup> B. H. Bransden, K. Smith, and C. Tate, *Proc. Roy. Soc. (London)* **A247**, 73 (1958).

† Work performed under the auspices of the U. S. Atomic Energy Commission.

Scattering of nucleons by tritium and  $\text{He}^3$  might be expected to be even more refractory mathematically than the three-nucleon problem. However, the current availability of electronic computers of higher speed and capacity than have been used before has reduced somewhat the technical difficulty of more detailed numerical calculations.

Nucleons can interact with mass-three nuclei in four ways:  $n$ -T,  $n$ - $\text{He}^3$  and  $p$ -T,  $p$ - $\text{He}^3$ . These correspond to the isobaric triad:  $\text{H}^4$ ,  $\text{He}^4$ ,  $\text{Li}^4$ . The middle pair of interactions differs significantly from the others in that there exists a strongly bound  $s$  state of that system of nucleons—the ground state of  $\text{He}^4$ .

Adequate experimental information on these four modes of interaction might permit conjoint analysis<sup>6</sup> in terms of parameters which are a function of isotopic spin, if the charge-independence hypothesis may be invoked.

### Previous Experiments

Extensive data are now available for the proton branches of this problem. For  $p$ -T elastic scattering absolute angular distributions have been measured at eleven energies between 1 and 2.5 Mev,<sup>7</sup> at seven energies between 2 and 3.5 Mev,<sup>8</sup> at 6.5 and 8.34 Mev,<sup>9</sup> and at 19.4 Mev.<sup>10</sup> For the  $p$ - $\text{He}^3$  case absolute angular distributions are available at four energies between 1 and 3.5 Mev,<sup>11</sup> at 5 Mev,<sup>12</sup> at 6.5 and 8.34 Mev,<sup>9</sup> at 9.75 Mev,<sup>13</sup> and at 19.4 Mev.<sup>10</sup>

No comparable data for the neutron branches has been available, although the total cross sections for  $n$ -T and  $n$ - $\text{He}^3$  interactions have been measured at numerous points between 0.2 and 22 Mev.<sup>14</sup> The only previous differential cross section measurement, for  $n$ -T scattering at 14 Mev,<sup>15</sup> is limited to scattering angles greater than  $80^\circ$ .

### Theoretical Work

Phase-shift analyses of the low-energy  $p$ -T and  $p$ - $\text{He}^3$  measurements<sup>7,8,11</sup> have been published.<sup>16,17</sup> The first detailed calculations of four-body scattering were made

by Swan.<sup>18</sup> The resonating group structure method<sup>19</sup> was employed and the scattering phases were evaluated by variational methods. Predictions were made for  $n$ -T and  $p$ - $\text{He}^3$  scattering for ordinary forces and for three mixtures of exchange forces. Comparison with the only available data<sup>15</sup> was inconclusive beyond suggesting that ordinary nonexchange forces were inadequate, as was expected. Subsequent comparison with  $p$ - $\text{He}^3$  scattering data<sup>11–13</sup> showed that the theory had failed to predict the strong backscattering observed. Furthermore, the calculated total cross section for  $n$ -T scattering was roughly a factor of two low compared to later measurements.<sup>14</sup>

In 1956 Bransden, Robertson, and Swan<sup>20</sup> published the results of a renewed attack on the problem, again using the resonating group formalism, but differing from the earlier work of Swan<sup>18</sup> in that certain inconsistencies in the earlier formalism were removed. Also, the exact solutions of the equations were obtained with the aid of a high-speed electronic computer. Predictions were made for  $n$ - $\text{He}^3$  and  $n$ -T scattering between 1 and 14 Mev. Calculations were carried out in detail only for the two cases that had led to acceptable, though inconclusive, results for nucleon-deuteron scattering, namely, the Serber and symmetrical exchange force mixtures. The differences between these two mixtures were found to be quite marked, unlike the results for nucleon-deuteron scattering in the earlier calculations. For each force mixture, the predictions for  $n$ -T and  $n$ - $\text{He}^3$  scattering are similar, but the Serber force produces much stronger forward and backward scattering at low energies. However, at 14 Mev the predictions of  $n$ -T scattering for the two mixtures are indistinguishable over the range of angles for which experimental data were available.

Comparison with the extensive data on total cross sections for these interactions<sup>14</sup> showed quite clearly (a) that the symmetrical mixture could account for only about half the total cross section in both cases, and (b) that the Serber mixture predicted the  $n$ -T total cross section within  $\pm 10\%$  above 1.5 Mev, and the  $n$ - $\text{He}^3$  elastic cross section almost as well above 2.5 Mev. These comparisons have been shown in Fig. 1 of reference 14 and in Fig. 7 of Bransden and Robertson's paper on  $p$ -T and  $p$ - $\text{He}^3$  scattering.<sup>21</sup> It is clear that the total cross section data strongly favor the Serber mixture.

In Fig. 1 are shown the calculated distributions for  $n$ -T scattering using the Serber mixture at the representative energies  $E_n=1, 2, 3.5$ , and 14 Mev. The  $n$ - $\text{He}^3$  results are quite similar.

In the experiments reported below complete sets of

<sup>6</sup> A. I. Baz', Zhur. Eksp. i Teoret. Fiz. **32**, 478 (1957) [translation: Soviet Phys.-JETP **5**, 403 (1957)].

<sup>7</sup> M. E. Ennis and A. Hemmendinger, Phys. Rev. **95**, 772 (1954).

<sup>8</sup> R. S. Claassen, R. J. S. Brown, G. D. Freier, and W. R. Stratton, Phys. Rev. **82**, 589 (1951).

<sup>9</sup> J. E. Brolley, T. M. Putnam, L. Rosen, and L. Stewart, Phys. Rev. **117**, 1307 (1960).

<sup>10</sup> R. A. Vanetsian and E. D. Fedchenko, Atomnaya Energ. **2**, 123 (1957) [translation: Soviet J. Atomic Energy **2**, 141 (1957)].

<sup>11</sup> K. F. Famularo, R. J. S. Brown, H. D. Holmgren, and T. F. Stratton, Phys. Rev. **93**, 928A (1954); and K. Famularo (private communication).

<sup>12</sup> D. R. Sweetman, Phil. Mag. **46**, 358 (1955).

<sup>13</sup> R. H. Lovberg, Phys. Rev. **103**, 1393 (1956).

<sup>14</sup> Los Alamos Physics and Cryogenics Groups, Nuclear Phys. **12**, 291 (1959).

<sup>15</sup> J. H. Coon, C. K. Bockelman, and H. H. Barschall, Phys. Rev. **81**, 33 (1951).

<sup>16</sup> J. S. McIntosh, R. L. Gluckstern, and S. Sack, Phys. Rev. **88**, 752 (1952).

<sup>17</sup> R. M. Frank and J. L. Gammel, Phys. Rev. **99**, 1406 (1955).

<sup>18</sup> P. Swan, Proc. Phys. Soc. (London) **A66**, 238 (1953); **A66**, 740 (1953).

<sup>19</sup> See reference 2, pp. 236ff.

<sup>20</sup> B. H. Bransden, H. H. Robertson, and P. Swan, Proc. Phys. Soc. (London) **A69**, 877 (1956).

<sup>21</sup> B. H. Bransden and H. H. Robertson, Proc. Phys. Soc. (London) **A72**, 770 (1958).

differential cross sections were obtained for the elastic scattering of neutrons by tritium and He<sup>3</sup> at  $E_n=1, 2, 3.5$ , and 6 Mev, together with polarization measurements at 1 and 2 Mev, to provide a more detailed test of the theory and as a guide for further calculations.

### TECHNIQUE

The technique of measurement represents a straightforward application of the pulsed-beam time-of-flight methods used previously—for example, in the study of  $n$ -d scattering.<sup>3</sup> The advantage of that method in improving the signal-to-background ratio proved to be of crucial importance for these measurements because of the unfavorable geometric configuration of the scatterers, the relatively small number of scattering nuclei, and the presence of relatively large amounts of containing and compounding material. The method was advantageous at all angles in discriminating against nonsynchronous background. At the larger angles, where one can resolve the scattering from T or He<sup>3</sup> completely from the synchronous background due to scattering by the heavier materials, the advantage is

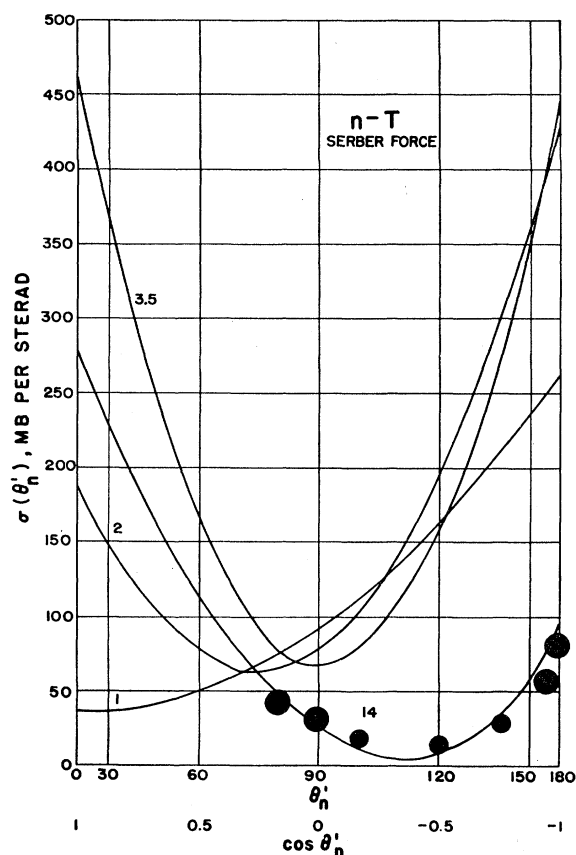


FIG. 1. Angular distributions for  $n$ -T scattering at  $E_n=1, 2, 3.5$ , and 14 Mev for the Serber force mixture, according to the calculations of B. H. Bransden, H. H. Robertson, and P. Swan. The data points are those of J. H. Coon *et al.* at 14 Mev (reference 15).

TABLE I. Relative forward yield  $Y$  of the  $T(p,n)He^3$  reaction, used in establishing the relative energy sensitivity of the neutron detector. Relative accuracy of any two points in the same region is  $\pm 3\%$ , and  $\pm 5\%$  for points below 1 Mev compared to points above 2 Mev.

$E_n$ , Mev	$Y$	$E_n$ , Mev	$Y$	$E_n$ , Mev	$Y$
0.25	0.477	1.02	0.507	3.00	0.886
0.30	0.417	1.25	0.596	3.50	0.785
0.38	0.422	1.50	0.724	4.00	0.630
0.47	0.426	1.75	0.869	4.50	0.518
0.62	0.469	2.00	0.963	5.08	0.417
0.76	0.485	2.25	1.000	5.50	0.375
0.84	0.490	2.50	1.000	6.00	0.315

particularly great. It should be noted, however, that despite these advantages the signal-to-background ratio for the least favorable situations, as at  $90^\circ$  at 6 Mev, was only 1:8.

### Apparatus and Calibration

The apparatus used in these measurements has been described.<sup>22</sup> The single detector system was used at all energies, and special runs on the sensitivity of the detector vs neutron energy were interspersed among the data runs. The detector sensitivity curve was obtained, as usual, by observing the counting rate of the detector vs neutron energy for neutrons produced at zero degrees by the reaction  $T(p,n)He^3$ . The forward yield curves to which our data are normalized are due to Perry and Haddad,<sup>23</sup> and Allen and Ferguson<sup>24</sup> for the neutron energy regions above 1 Mev and below 2 Mev, respectively. The curves of Perry and Haddad and of Allen and Ferguson have been normalized to each other in the region of overlap from 1 to 2 Mev. The relative shape of the combined data is given in Table I. Changes in the values of Table I which may be indicated by future measurements would modify our results in a corresponding way.

The  $T(p,n)He^3$  reaction was used as the neutron source for the scattering measurements at the three lowest energies, and the  $D(d,n)He^3$  source was used to obtain the 6-Mev data.

Cross section determinations were made by comparison with  $n$ -p scattering using a thin shell of CH<sub>2</sub> as the scatterer.

The flight path from the center of the sample to the center of the detector was typically 1.17 m. Representative time spectra obtained under these conditions are illustrated in Figs. 2 and 3.

### Samples

The pressure vessel used to contain He<sup>3</sup> was made out of Armco 17-7 PH stainless steel, with inside diameter

<sup>22</sup> L. Cranberg and J. S. Levin, Phys. Rev. **103**, 343 (1956).

<sup>23</sup> J. E. Perry, Jr. and E. Haddad, Los Alamos Scientific Laboratory (private communication).

<sup>24</sup> W. D. Allen and A. T. Ferguson, Atomic Energy Research Establishment, Harwell (private communication).

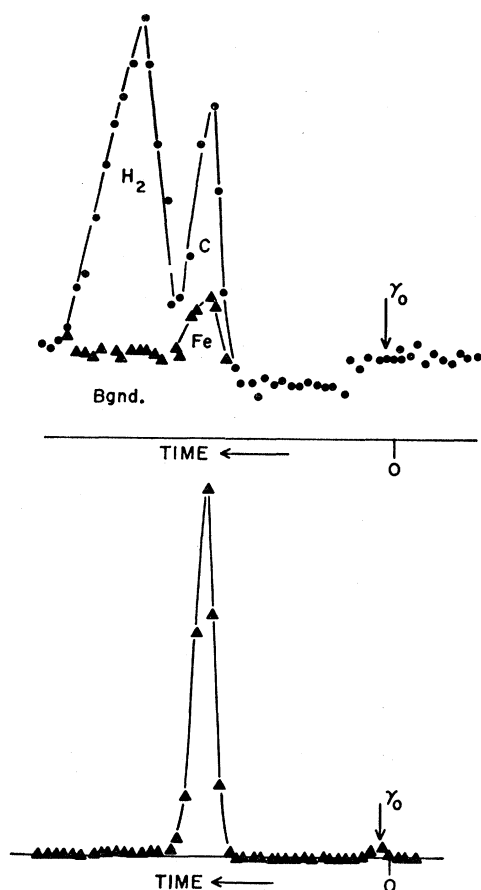


FIG. 2. Time-of-flight spectra at  $E_n = 3.5$  Mev. Lower: Neutrons incident on the scattering samples. Points labeled  $\gamma_0$  are  $\gamma$  rays produced in the target gas cell. Upper: Neutrons recoiling from the  $\text{CH}_2$  calibration sample at  $30^\circ$  to the incident neutron direction, showing resolution of the two components. Synchronous portion of the background labeled Fe is from steel cable supporting the sample.

1.5 in. and walls 0.034 in. thick. The pressure used was 4750 psi. At this pressure the sphere contained about one-third mole of  $\text{He}^3$ , at about one-third the density of liquid  $\text{He}^3$ . The ratio of  $\text{He}^3$  nuclei to steel nuclei in the sample was about 1:1.

Welded to the sphere was a length of capillary tubing for filling and for monitoring the pressure. A precise pressure gauge was connected to the cell so that a continuous check could be made of the cell pressure. No loss of gas was observed over the several months of observation.

A light-weight frame was constructed to support the cell and gauge, and on this same frame three other samples were supported: an identical evacuated steel cell, a third cell filled with  $\text{He}^4$  at 5000 psi and its monitoring gauge, and a thin-walled shell of  $\text{CH}_2$ . By displacing the frame vertically the appropriate sample could be brought into position in front of the neutron source. The  $\text{CH}_2$  was in the form of a spherical shell of inside diameter 1 in. and thickness 0.055 in.

The tritium sample was prepared in the form of  $\text{CaT}_2$ . Calcium proved to be the most suitable choice of compounding material taking into account the following considerations: ease of preparation of the compound, ease of preparation of a sample of the compounding material itself, low density of nuclear levels up to 6 Mev, low elastic scattering cross section, and high tritium density. The compound was prepared *in situ* in a sample container which had been filled with granulated calcium. Tritiation for several hours at  $600^\circ\text{C}$  resulted in a mixture of Ca and  $\text{CaT}_2$  which averaged  $\text{CaT}_{1.56}$ .

The container was of Type 347 stainless steel, with inside diameter 1.25 in. and wall thickness 0.010 in. After loading with calcium through a small hole, a thin-walled steel tube about 10 in. long was welded on and used for filling the sphere with the tritium gas. The tube was terminated by a light-weight valve which could be opened to bleed off the  $\text{He}^3$  which evolved from the decay of the tritium. The tritium activity was about 20 000 curies, and the calculated generation of  $\text{He}^3$  was at a rate of about 1 cc at NTP per day. Sufficient free volume was available in the sphere to make venting unnecessary at intervals of less than several

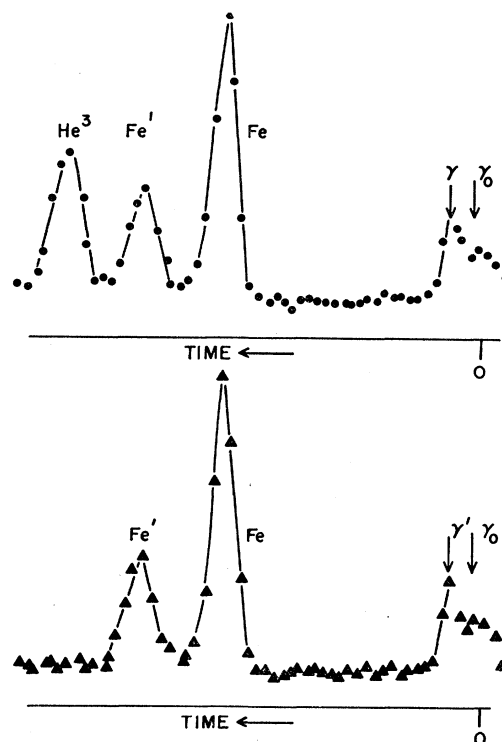


FIG. 3. Time-of-flight spectra at  $E_n = 2$  Mev from the gas cells at  $120^\circ$ . Lower: Fe and Fe' are the elastic and inelastic neutron groups from the evacuated dummy cell.  $\gamma_0$  is the  $\gamma$  ray from the source, and  $\gamma'$  the  $\gamma$  ray from inelastic scattering, delayed by the flight time of the incident neutrons. Upper: Corresponding neutrons from the cell filled with high-pressure  $\text{He}^3$ , showing complete resolution of the group due to  $\text{He}^3$ .

weeks.<sup>25</sup> The sample contained about  $\frac{1}{2}$  mole of tritium,  $\frac{1}{3}$  mole of calcium, and  $\frac{1}{8}$  mole of steel. It was warm to the touch.

A light-weight wire frame supported the sample, an identical evacuated sphere, a third sphere filled with an amount of calcium equal to that in the sample, and a thin-walled shell of CH<sub>2</sub>. This framework also could be displaced vertically to position the various samples relative to the neutron source and detector.

### Procedure

Complete time spectra were obtained for each run. At the beginning and end of each day's running a check was made of the yield from the CH<sub>2</sub> scatterer. The neutron source was continuously monitored by means of a "long counter" to check on the stability of the target.

For the case of tritium, backgrounds were obtained using the evacuated sphere and the calcium-filled sphere. For the He<sup>3</sup> case only the evacuated sphere background was taken regularly. For both samples an occasional "blank" background was necessary to unravel the contribution to the elastic scattering of the various components of the sample. The target-to-scatterer distance was checked frequently. For the He<sup>3</sup> runs the distance from the center of the scatterer to the center of the target was 6 in. For the smaller tritium sample this distance was reduced to 5 in.

### TREATMENT OF THE DATA

#### Backgrounds

It was necessary to determine the sample-independent background before applying corrections for multiple scattering and self-absorption, even though the masses of steel and calcium in the dummy spheres were made identical to their respective masses in the sample spheres. The time channels of interest were determined by inspection of superimposed plots of sample and dummy data. The sample-independent portion could usually be inferred from interpolation between the data points lying just outside the region of interest. Where necessary, a "sample out" measurement was made. This background was subtracted from both sets of data to obtain preliminary "net" sample and dummy numbers, to which the corrections could be applied.

#### Monte Carlo Calculations

In order to make sufficiently accurate corrections for self-absorption and multiple scattering, a detailed Monte Carlo calculation<sup>26</sup> was made for each sample

<sup>25</sup> The rate of He<sup>3</sup> released from metallic tritides is much lower than expected when the materials are first made, apparently due to trapping in the crystal structure. Our CaT<sub>2</sub> sample did not approach the equilibrium rate for several months.

<sup>26</sup> E. D. Cashwell and C. J. Everett, *A Practical Manual for the Monte Carlo Method for Random Walk Problems* (Pergamon Press, New York, 1959).

and at each energy corresponding to experiment. Adequate experimental information was available for all the cross sections required in the calculations either from previous measurements or from the preliminary results of our measurements. The total cross section of calcium was measured in an ancillary experiment.<sup>27</sup> The elastic angular distributions for calcium were obtained incidental to the *n*-T results. For the tritium and He<sup>3</sup> cross sections preliminary experimental angular distributions were normalized to the known elastic cross section at the four energies of measurement with interpolation guided by the theory for the Serber force. In the same manner the optical model calculation of Beyster *et al.*<sup>28</sup> was used for interpolation between the iron and calcium cross sections previously known or measured in this experiment.

Calculations were carried out for each of the 24 experimental situations. These followed the history of between 60 000 and 140 000 of the incident neutrons that made at least one collision in the sample.

For each experimental situation, energy limits were specified to correspond to the experimentally observed neutron groups, and the calculations gave the relative numbers of neutrons falling between those limits which had been scattered either once or more than once. These numbers were used to make corrections for multiple scattering. The flux was averaged over those cases detected as single scatterings; these values were used to make the corrections for absorption in the samples. Since an identical procedure was used in reducing the data from the CH<sub>2</sub> sample taken under identical conditions, the absolute flux and solid angles were not required and only the *relative* sensitivities for the neutron energies corresponding to the hydrogen calibration and to the data points in question were needed.

### DISCUSSION OF ERRORS

#### Statistics and Backgrounds

Between 10 000 and 100 000 counts were recorded in the sample data channels for each observation and the statistical standard deviation (s.d.) in the corrected net differences between sample and dummy runs ranged from about 2% in favorable well-resolved cases up to a maximum of 9% in cases where the scattering of interest could not be resolved in time from the strong forward scattering from calcium or iron. A dummy run includes two components: the contribution of the dummy cell, and the background in the absence of the sample. Since this background is subtracted from the sample and dummy counts *before* the differences are corrected for self-absorption and multiple scattering, any error in the estimation of its magnitude would be propagated as an error in the net effect. The possible

<sup>27</sup> L. Cranberg, J. D. Seagrave, and J. E. Simmons, *Bull. Am. Phys. Soc.* **3**, 336 (1958). Abstracts of preliminary reports on the *n*-T and *n*-He<sup>3</sup> work appear on p. 338.

<sup>28</sup> J. R. Beyster *et al.*, Los Alamos Scientific Laboratory Report LA-2099, 1955 (unpublished).

error due to this uncertainty was computed as 10% of the background value, multiplied by the difference in correction factors applied to the sample and dummy values. This error was generally quite negligible except for the same unfavorable cases mentioned above and also for the very low cross sections near the minimum in  $n\text{-He}^3$  scattering at 6 Mev.

### Sensitivity and Drifts

The sensitivity curve of our detector rises from a threshold set by electronic means at about 200 kev, to a maximum near 800 kev, and then decreases monotonically with increasing energy.<sup>29</sup> The estimated s.d. in the relative sensitivity curve was based on statistics and reproducibility of the data calibration points. It was typically 1% to 2% for most of the points required, and increased to about 4% for points lying on the low-energy portion of the curve, namely, those for backward angles at 1-Mev bombarding energy.

A possible error arising from uncompensated drifts in target pressure or electronic equipment, or from changes in the operation of the accelerator, was estimated at not more than one percent of the background, and this numerical value was used as an s.d. for stability. It became the dominant uncertainty only at the two smallest angles for  $n\text{-T}$  scattering at 1 Mev.

### Monte Carlo Calculations

Since the Monte Carlo mode of calculation is a statistical process, the results of such calculations themselves have a statistical uncertainty. However, the numbers actually computed for the multiple-scattering groups had an s.d. of less than 5% and the magnitude of the correction applied to the data was typically 3% to 5%, ranging up to a maximum of 20% at the most unfavorable cases. The uncertainty in the final cross section arising from this source was in all cases less than 1% and in particular was entirely negligible compared to other sources of error at corresponding points. The total correction applied to the data for flux attenuation and multiple scattering never exceeded 9% and was typically 3% to 5%.

### Sample Composition

The composition of the  $\text{He}^3$  gas was analyzed<sup>30</sup> and found to contain 0.31% of  $\text{He}^4$ , and negligible quantities of the hydrogen isotopes. No correction was made for these contaminants. The content of the sphere was computed from a plot of Amigat density vs pressure<sup>31</sup> and  $PVT$  measurements. The sphere was found to contain  $0.341 \pm 0.007$  moles of  $\text{He}^3$ .

The calcium tritide sample was loaded with  $0.514 \pm 0.005$  atomic moles of tritium contaminated with

less than 0.2% hydrogen.<sup>32</sup> The quantity given was determined to about 1% by inventory of the tritium content of the rest of the system before and after filling. This is actually an upper limit to the sample content since it is possible that some tritium left the system by diffusion through the thin steel walls of the sample which was maintained at about 600°C for about 8 hours. It is felt that not over 1% could have been lost in this manner since the corresponding activity (200 curies) should have been detectable over background in the exhaust even if spread uniformly over this period.

The tritium results are affected by an uncertainty due to nonuniform loading of the sample. Both sample and dummy cells were loaded as uniformly as possible with equal amounts of calcium from the same source of finely granulated material. It was found necessary to do the tritium loading at an elevated temperature with the axis of the sample horizontal. Apparently, in the process of forming the tritide some of the calcium crystals divided into a finer powder and sifted downward and packed more densely. Also, since only 78% of the stoichiometric reaction was formed, it is likely that some of the finer grains toward the bottom went completely to  $\text{CaT}_2$  and some of the larger grains left behind reacted less than the average. Judging from experience with calcium hydride samples prepared in this fashion which were subsequently dissected, the sample ultimately sinters into a porous ceramic material and our sample should have been mechanically stable when the reaction was terminated. This eccentricity of loading was anticipated on the basis of radiography of the sample and investigated experimentally by observing at a favorable angle the  $n\text{-T}$  scattering as a function of the angle of orientation of the sample with respect to the source. This type of observation was made at two energies and angles. A mean correction of  $(5 \pm 4)\%$  was indicated for the tritium data, and such a correction was applied in preliminary reduction of the data. Comparable data for the calcium was not obtained. To reduce the uncertainty corresponding to this effect, least-squares fits were made to the preliminary data, and the integrated cross sections compared with the known  $n\text{-T}$  total cross sections  $\sigma_T$ . It was found that the preliminary integrals were slightly low compared to  $\sigma_T$  and that the discrepancy was in the direction to be expected if the correct value of eccentricity were larger than the one used. By an iterative procedure the eccentricity value was adjusted to a final value of  $(7 \pm 3)\%$  to give best agreement with the total cross sections. The possibility of making such an adjustment partially by a change in the eccentricity and partially by a change in the number of atoms of tritium present was investigated and found to give differential cross-section values lying within the standard deviations calculated by the procedure described above.

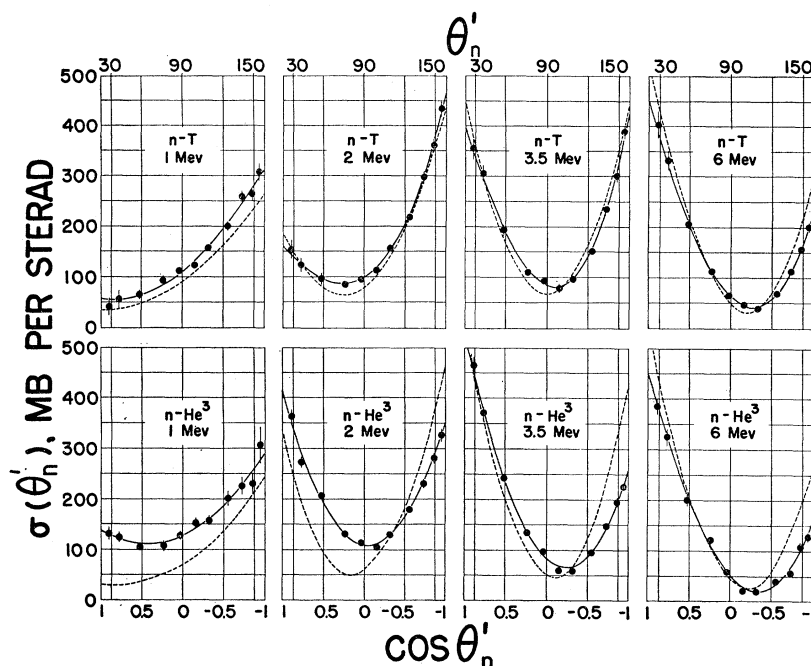
<sup>29</sup> See Fig. 2 of reference 22.

<sup>30</sup> The  $\text{He}^3$  sample filling and analysis was performed by R. H. Sherman and F. Edeskuty.

<sup>31</sup> A. Michels and H. Wouters, *Physica* 8, 923 (1941).

<sup>32</sup> The tritium sample filling and analysis was arranged by A. C. Briesmeister.

FIG. 4. Differential cross sections for the elastic scattering of fast neutrons by tritium and He<sup>3</sup> at  $E_n=1, 2, 3.5$ , and 6 Mev. The solid curves are least-squares fits to the data, and the dashed curves are the predictions of B. H. Bransden, H. H. Robertson, and P. Swan (reference 20).



### Resolution and Geometry

The target thicknesses were generally chosen to give a full neutron energy spread from the target of about 100 keV except for  $n$ -T scattering at 1 MeV where it was increased to 200 keV to get sufficient intensity to measure the small forward cross sections. The over-all resolution is primarily due to the time resolution of the apparatus at the two higher energies, and to the effects of geometry and energy spread in the primary neutrons at the two lower energies.

The samples were placed as close to the target as possible without introducing serious geometrical uncertainties. The spherical samples subtended a full angle of 14° at the target center which introduced a mean uncertainty of  $\pm 5^\circ$  in scattering angles. No correction for finite angular resolution was applied to the data since at no point does a possible error due to this cause appear to be comparable with the standard deviation from other sources.

The s.d. in the cross-section scale as determined by the CH<sub>2</sub> measurements was typically 2%.

For each data point all of the above errors associated with various corrections and calibrations were combined with the statistical s.d. as random errors—that is to say, the square root of the sum of the squares of the contributing errors was calculated and that value used as the over-all standard deviation.

### ANGULAR DISTRIBUTIONS

The absolute differential cross sections determined in this experiment are collected in Table II and presented graphically in Fig. 4 in comparison with the

predictions of the theory<sup>20</sup> for the Serber force. In Table II the absolute center-of-mass differential cross sections are tabulated together with the cosine of the center-of-mass scattering angle  $\theta'$ . The c.m. cross sections are plotted in Fig. 4 as a function of  $\cos \theta'$ , as the corresponding curves are then very close to simple parabolas (see below). In the figures the solid curves

TABLE II. Absolute differential cross sections in the c.m. system for elastic scattering of fast neutrons by tritium and He<sup>3</sup>, with their standard deviations (s.d.). Values may be multiplied by the ratio  $\sigma/\sigma'$  to obtain the laboratory cross section at the laboratory angle  $\theta$ .

$\theta$	$E_n$ : $\theta'$	1 Mev $\sigma'$	2 Mev $\sigma'$	3.5 Mev $\sigma'$	6 Mev $\sigma'$	$\sigma/\sigma'$	$\cos \theta'$
degrees		millibarns per steradian (c.m.)					
Tritium:							
0°	0	59 ± 11	162 ± 34	401 ± 45	456 ± 16	1.781	1.000
20	26.6	42 ± 18	153 ± 18	356 ± 23	404 ± 28	1.721	0.894
30	39.6	57 ± 16	124 ± 15	307 ± 19	334 ± 18	1.650	0.770
45	58.7	66 ± 7	96 ± 11	195 ± 11	207 ± 9	1.502	0.519
60	76.8	94 ± 8	85 ± 3	111 ± 6	113 ± 5	1.321	0.228
70	88.3	113 ± 5	95 ± 4	93 ± 6	66 ± 3	1.192	0.030
80	99.1	124 ± 6	114 ± 5	80 ± 7	47 ± 3	1.065	-0.157
90	109.5	158 ± 7	157 ± 6	96 ± 6	40 ± 3	0.9423	-0.334
105	123.8	203 ± 8	218 ± 7	152 ± 6	69 ± 4	0.7811	-0.556
120	136.8	260 ± 11	298 ± 11	235 ± 7	113 ± 5	0.6520	-0.729
135	148.7	265 ± 13	361 ± 13	301 ± 10	157 ± 7	0.5559	-0.855
152	161.0	310 ± 18	436 ± 16	389 ± 13	201 ± 8	0.4854	-0.946
180°	180.0	319 ± 11	459 ± 34	419 ± 45	227 ± 16	0.4429	-1.000
He <sup>3</sup> :							
0°	0	138 ± 14	415 ± 11	526 ± 7	442 ± 28	1.781	1.000
20	26.6	133 ± 12	365 ± 14	464 ± 16	386 ± 18	1.721	0.894
30	39.6	126 ± 10	273 ± 10	371 ± 11	325 ± 17	1.650	0.770
45	58.7	106 ± 6	208 ± 5	242 ± 8	200 ± 11	1.502	0.519
60	76.8	109 ± 8	132 ± 5	135 ± 6	122 ± 10	1.321	0.228
70	88.3	128 ± 8	114 ± 4	98 ± 6	59 ± 7	1.192	0.030
80	99.1	153 ± 9	106 ± 5	60 ± 6	22 ± 6	1.065	-0.157
90	109.5	158 ± 9	127 ± 6	59 ± 6	20 ± 6	0.9423	-0.334
105	123.8	202 ± 15	181 ± 7	95 ± 8	39 ± 7	0.7811	-0.556
120	136.8	225 ± 17	232 ± 8	147 ± 6	57 ± 7	0.6520	-0.729
135	148.7	230 ± 22	282 ± 10	195 ± 8	110 ± 9	0.5559	-0.855
152	161.0	306 ± 37	328 ± 13	226 ± 6	128 ± 9	0.4854	-0.946
180°	180.0	291 ± 14	351 ± 11	259 ± 7	155 ± 28	0.4429	-1.000

<sup>a</sup> 0° and 180° values are from least-squares fits.

TABLE III. Legendre polynomial coefficients  $C_n$  and  $B_n$  of the expansions  $\sigma(\mu) = \sum_0^3 C_n P_n(\mu)$  and  $k^2\sigma(\mu) = \sum_0^3 B_n P_n(\mu)$ . Uncertainties shown are standard deviations from the internal goodness-of-fit. Absolute error is  $\pm 3\%$ .

Cross-section expansions (millibarns per steradian)					$k^2\sigma$ expansions				
$E_n$ :	1 Mev	2 Mev	3.5 Mev	6 Mev	$E_n$ :	1 Mev	2 Mev	3.5 Mev	6 Mev
Tritium					Tritium				
$C_0$	$137 \pm 5$	$168 \pm 2$	$192 \pm 4$	$155 \pm 2$	$B_0$	$0.37 \pm 0.01$	$0.91 \pm 0.01$	$1.83 \pm 0.04$	$2.53 \pm 0.03$
$C_1$	$-127 \pm 6$	$-126 \pm 8$	$26 \pm 14$	$132 \pm 6$	$B_1$	$-0.34 \pm 0.02$	$-0.68 \pm 0.04$	$0.24 \pm 0.13$	$2.15 \pm 0.10$
$C_2$	$50 \pm 7$	$143 \pm 4$	$218 \pm 6$	$186 \pm 4$	$B_2$	$0.13 \pm 0.02$	$0.78 \pm 0.02$	$2.08 \pm 0.06$	$3.04 \pm 0.06$
$C_3$	...	$-22 \pm 4$	$-34 \pm 7$	$-17 \pm 3$	$B_3$	...	$-0.12 \pm 0.02$	$-0.33 \pm 0.06$	$-0.28 \pm 0.05$
$\text{He}^3$					$\text{He}^3$				
$C_0$	$156 \pm 5$	$201 \pm 4$	$186 \pm 4$	$134 \pm 5$	$B_0$	$0.42 \pm 0.01$	$1.09 \pm 0.02$	$1.77 \pm 0.04$	$2.19 \pm 0.09$
$C_1$	$-76 \pm 5$	$32 \pm 5$	$144 \pm 13$	$167 \pm 17$	$B_1$	$-0.21 \pm 0.01$	$0.17 \pm 0.03$	$1.37 \pm 0.13$	$2.72 \pm 0.28$
$C_2$	$58 \pm 7$	$182 \pm 6$	$206 \pm 6$	$164 \pm 7$	$B_2$	$0.16 \pm 0.02$	$0.99 \pm 0.03$	$1.96 \pm 0.05$	$2.68 \pm 0.12$
$C_3$	...	...	$-10 \pm 6$	$-17 \pm 8$	$B_3$	...	...	$-0.10 \pm 0.06$	$-0.28 \pm 0.13$

correspond to the least-squares fits and the dashed curves are the predictions of the theory. It will be observed that the theory provides a representation of  $n$ -T scattering which is generally excellent at all four energies. It should be realized that not even total cross sections were known to the theorists at the time the calculations were made. The similarity between  $n$ -T and  $n$ - $\text{He}^3$  scattering is not found as marked as the theory suggested, and there is a discrepancy outside experimental error between theory and experiment for all four sets of observations, although the qualitative features of the distributions are predicted correctly. In general, the experimental curves have minima occurring at a larger angle and with a greater cross section than predicted.

Least-squares fits to the data were made using a procedure<sup>33</sup> which permitted the square of the difference between experimental and fitted point to be weighted inversely as the square of the experimental s.d., point by point. Fits were evaluated for between three and seven terms of Legendre and power series expansions in  $\cos\theta'$ , and the standard deviations of the coefficients were evaluated from internal consistency. Only three terms were found to be significant for both cases at 1 Mev and for  $n$ - $\text{He}^3$  at 2 Mev. Four terms were required for the other cases. The results for the Legendre expansions are given in Table III, together with the corresponding values of expansions of  $k^2\sigma$ . The latter terms are more closely related to the nuclear phase shifts.<sup>34</sup> These are plotted as a function of energy in Fig. 5. With the aid of the least-squares coefficients the cross section values at  $0^\circ$  and  $180^\circ$  were calculated, and these have been included in Table II. The best determination of the integrated elastic cross section  $\sigma_e$  is given by the least-squares analysis, since  $\sigma_e = 4\pi C_0$ , where  $C_0$  is the zero-order Legendre term. The values derived from our measurements are presented in Table IV and compared with the values of  $\sigma_T$  from the direct measurements of reference 14. The s.d. given for  $\sigma_e$  are in a few cases

relatively larger than those for the corresponding values of  $C_0$  in Table III, since the latter are derived from internal consistency; the s.d. for  $\sigma_e$  reflect the absolute scale uncertainty. These cross sections are plotted in Fig. 6, together with all the data of reference 14.

For  $\text{He}^3$ , the nonelastic cross sections  $\sigma_{ne}$  were obtained from the relation  $\sigma_{ne} = \sigma_T - \sigma_e$ . Also shown in Fig. 6 are the  $\text{He}^3(n,p)\text{T}$  and  $\text{He}^3(n,d)\text{D}$  cross sections derived from the best available experimental data for the inverse reactions,<sup>35</sup> using the theorem of detailed balance.

## POLARIZATION

### Introduction

To investigate the role of spin-orbit or tensor forces in nuclear scattering one may investigate the scattering of spin-oriented or polarized neutrons. In the calculations<sup>20</sup> with which our results have been compared these forces were neglected, but it was thought worthwhile to make polarization measurements in anticipa-

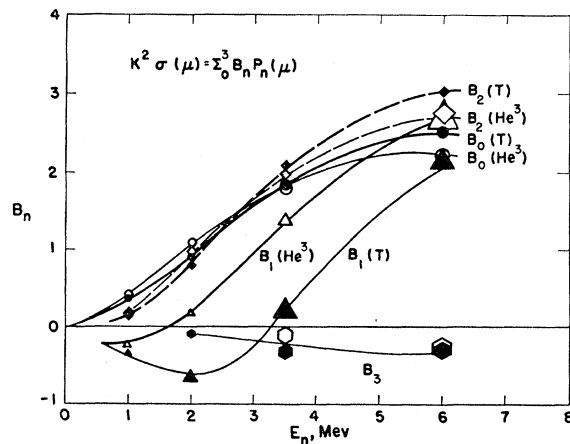


FIG. 5. Coefficients in the Legendre series expansion of  $k^2\sigma$  for  $n$ -T and  $n$ - $\text{He}^3$  scattering between  $E_n = 1$  and 6 Mev.

<sup>33</sup> Los Alamos IBM 704 Subroutine M-050.

<sup>34</sup> The square of the wave number,  $k^2 = 2.72 E$  barns<sup>-1</sup> Mev<sup>-1</sup> for a neutron of laboratory energy  $E$  incident on a target of T or  $\text{He}^3$ .

<sup>35</sup> J. D. Seagrave, in *Proceedings of the Conference on Nuclear Forces and the Few-Nucleon Problem, London, 1959* (Pergamon Press, New York, 1960).



tion of more refined calculations. An additional experiment was undertaken to study the scattering of 1- and 2-Mev polarized neutrons by T and He<sup>3</sup>.

Other investigations have demonstrated that 1-Mev neutrons from the Li<sup>7</sup>(*p,n*)Be<sup>7</sup> reaction at 50° in the laboratory are 30% polarized<sup>36</sup> and that 2-Mev neutrons at 35° are 35% polarized.<sup>37</sup> The procedure used in measuring the polarization of neutrons scattered by T and He<sup>3</sup> was substantially identical to that described in reference 37.

### Results

A preliminary check on the polarization of neutrons produced by the Li<sup>7</sup>(*p,n*)Be<sup>7</sup> reaction was made at 1.10 and 2.15 Mev, using *n*-He<sup>4</sup> scattering as the analyzer.<sup>37</sup> The results are given in Table V. They are consistent with the more precise values reported earlier at nearby energies, namely  $P = 0.30 \pm 0.02$  at  $E_n = 980$  kev<sup>36</sup> and  $P = 0.38 \pm 0.03$  at  $E_n = 2.09 \pm 0.05$  Mev<sup>37</sup> at the corresponding angles 50° and 35°, respectively. These latter values were adopted as the source polarization for further measurements.

The *n*-He<sup>4</sup> polarizations were calculated from the phase shifts of Dodder and Gammel<sup>38</sup> and of Seagrave.<sup>39</sup> At 1.10 Mev the uncertainty is primarily due to the energy and angular spread in our experiment, and at 2.15 Mev it is largely due to the uncertainty in the  $P_2$  phase shift.<sup>39,40</sup>

TABLE IV. Comparison with independent total cross sections  $\sigma_T$  of the elastic cross sections  $\sigma_e$  for *n*-T and *n*-He<sup>3</sup> scattering obtained by integration of the differential cross sections. For He<sup>3</sup>, the nonelastic cross section  $\sigma_{ne} = \sigma_T - \sigma_e$ .

$E_n$	1 Mev	2 Mev	3.5 Mev	6 Mev
<i>n</i> -T				
$\sigma_T^a$	$1.70 \pm 0.05$	$2.08 \pm 0.05$	$2.47 \pm 0.05$	$2.02 \pm 0.05$
$\sigma_e$	$1.72 \pm 0.06$	$2.10 \pm 0.06$	$2.41 \pm 0.07$	$1.95 \pm 0.06$
<i>n</i> -He <sup>3</sup>				
$\sigma_T^a$	$2.87 \pm 0.06$	$3.25 \pm 0.06$	$2.77 \pm 0.06$	$2.16 \pm 0.06$
$\sigma_e$	$1.96 \pm 0.06$	$2.52 \pm 0.07$	$2.34 \pm 0.06$	$1.69 \pm 0.07$
$\sigma_{ne}$	$0.91 \pm 0.09$	$0.73 \pm 0.09$	$0.43 \pm 0.09$	$0.47 \pm 0.09$

<sup>a</sup> Total cross sections from a smooth curve through the data of reference 14. Cross sections are in barns, with absolute standard deviations indicated.

TABLE V. Polarization  $P_1$  of Li<sup>7</sup>(*p,n*)Be<sup>7</sup> neutrons of energy  $E_n$  emitted at a laboratory angle  $\theta_1$  as measured by *n*-He<sup>4</sup> scattering at a laboratory angle  $\theta_2$  and c.m. angle  $\theta_2'$ . Positive polarization is here taken to mean spin in the direction  $\mathbf{k}_{in} \times \mathbf{k}_{out}$ .  $P_2$  is the calculated polarization for *n*-He<sup>4</sup> scattering. A positive product  $P_1 P_2$  corresponds to preferential scattering to the left.

$E_n$ (Mev)	$\theta_1$	$\theta_2$	$\theta_2'$	$P_2$	$P_1 P_2$	$P_1$
$1.10 \pm 0.07$	50°	75°	89°	$0.69 \pm 0.07$	$0.185 \pm 0.005$	$0.27 \pm 0.03$
$2.15 \pm 0.05$	35°	106°	120°	$0.75 \pm 0.05$	$0.32 \pm 0.04$	$0.42 \pm 0.08$

<sup>36</sup> H. R. Striebel, S. E. Darden, and W. Haeberli, Nuclear Phys. 6, 188 (1958).

<sup>37</sup> L. Cranberg, Phys. Rev. 114, 174 (1959).

<sup>38</sup> D. C. Dodder and J. L. Gammel, Phys. Rev. 88, 520 (1952).

<sup>39</sup> J. D. Seagrave, Phys. Rev. 92, 1222 (1953).

<sup>40</sup> I. I. Levintov, A. V. Miller, and V. N. Shamshev, Nuclear Phys. 3, 221 (1957).

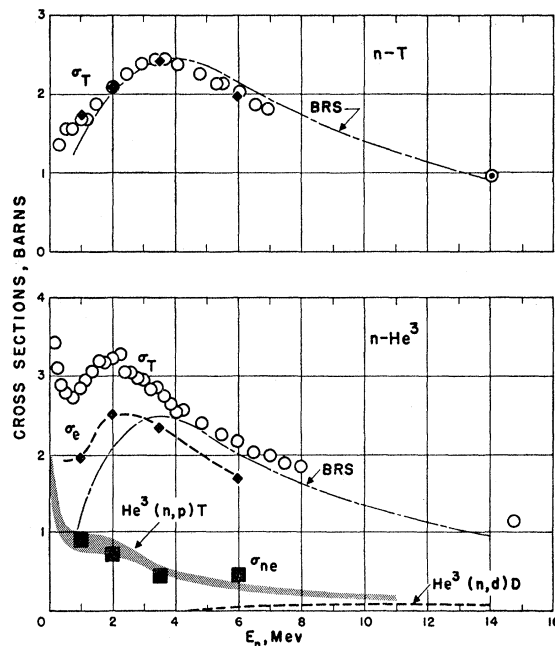


FIG. 6. Integrated cross sections for the interaction of fast neutrons with tritium and He<sup>3</sup>, including total cross sections  $\sigma_T$  from reference 14, the elastic and nonelastic cross sections  $\sigma_e$  and  $\sigma_{ne}$  of this work (Table IV), the He<sup>3</sup>(*n,p*)T reaction and the He<sup>3</sup>(*n,d*)D reaction from detailed balance calculations (reference 35), and the theory (BRS) of reference 20.

The results for the polarization of neutrons scattered by T and He<sup>3</sup> are presented in Table VI. The results are generally consistent with negligible polarization within our uncertainties of 4% to 12%, and the greatest departure from a value of zero polarization is only 1.5 standard deviations. Fluctuations of this order are to be expected, and were observed in the several individual measurements which were combined in the more precisely determined values at  $\theta' = 94^\circ$ . The latter are, moreover, closer to zero polarization than any of the single observations.

In view of the small size of the effects observed, the elaborate calculations required for multiple-scattering and source-anisotropy corrections were not attempted. Rough estimates of these effects indicated that they should be less than the quoted errors. The corrections would be positive in sense, which would reduce the spread about a value of zero.

These results may be regarded as consistent with the calculations of Bransden *et al.*<sup>20</sup> based on central forces and undistorted wave functions. More refined measurements than these will be required to obtain direct evidence for the role of spin-orbit or tensor forces in neutron scattering by T and He<sup>3</sup>.

### DISCUSSION AND CONCLUSION

The agreement of theory with experiment shown in Fig. 4 is quite striking for the case of *n*-T scattering, particularly when it is noted that no adjustment of

TABLE VI. Polarization  $P_2$  of neutrons scattered by T and  $\text{He}^3$  at laboratory angles  $\theta_2$  and c.m. angles  $\theta_2'$ .  $P_1$  is the polarization of incident neutrons from the  $\text{Li}^7(p,n)\text{Be}^7$  source.

$E_n$ (Mev)	Target	$\theta_2$	$\theta_2'$	$P_1$	$P_1 P_2$	$P_2$
1.10	T	65°	83°	0.30 ± 0.02 <sup>a</sup>	0.031 ± 0.019	0.10 ± 0.07
1.10	T	75°	94°	0.30 ± 0.02	-0.010 ± 0.012 <sup>b</sup>	-0.03 ± 0.04 <sup>b</sup>
1.10	T	102°	121°	0.30 ± 0.02	-0.014 ± 0.020	-0.05 ± 0.07
1.10	$\text{He}^3$	75°	94°	0.30 ± 0.02	0.003 ± 0.008 <sup>b</sup>	0.01 ± 0.03 <sup>b</sup>
1.10	$\text{He}^3$	102°	121°	0.30 ± 0.02	-0.057 ± 0.030	-0.19 ± 0.12
2.15	$\text{He}^3$	120°	137°	0.38 ± 0.03 <sup>a</sup>	-0.025 ± 0.023	-0.07 ± 0.07

<sup>a</sup> Values of  $P_1$  are those of references 36 and 37.

<sup>b</sup> Weighted averages of several runs.

parameters to "fit" the data was involved, as is common with the optical model, for example. The differences that exist are small and systematic, and it is plausible to expect that a phenomenological interaction of similar form should be capable of representing the data within its stated errors. The pure Serber force would produce no polarization, and it might be inferred that such small "adjustments" would not produce polarizations at variance with our measurements of small degrees of polarization. Hochberg has found<sup>41</sup> that the use of the force previously employed to describe nucleon- $\text{He}^4$  scattering<sup>42</sup> in which the exchange force mixture was nine-tenths Serber and one-tenth symmetrical, with a spin-orbit term chosen to give correctly the  $p$ -state splitting, gives better absolute agreement with the  $n$ -T data at 1 Mev than does the simple Serber force, but at the cost of introducing irregularities in the distribution which do not seem compatible with experiment. Hochberg's mixture does *not* produce polarization in this case, since the contributions of the different spin states average to zero.<sup>41</sup>

The agreement in the case of  $n$ - $\text{He}^3$  scattering is poorer, although theory seems to indicate qualitatively the general shape and trend with energy of the distributions. In the published calculations, only elastic scattering was considered, although in fact the  $\text{He}^3(n,p)\text{T}$  and  $\text{He}^3(n,d)\text{D}$  reactions are quite important, as shown in Fig. 6. At the two higher energies, the better agreement noted in Fig. 4 may be due in part to the smaller fractional competition of the reaction channels. The effect seems to be primarily one of reducing the contribution to backscattering, which is qualitatively reasonable if the reactions are interpreted as charge-exchange interactions which compete with the space-exchange interactions. The latter are associated with the characteristic backscattering peak in the scattering of nucleons by the very light nuclei. It is to be expected that the scattering amplitudes, which contain terms of the form  $e^{2i\delta}$  when only elastic scattering is possible, will contain corresponding terms of the form  $\alpha e^{2i\delta}$  which are of amplitude  $|\alpha| < 1$  due to the competition of the reaction channels. This effect will reduce the cross sections even if the phases  $\delta$  are approximately correct.

<sup>41</sup> S. Hochberg, Imperial College, London, England (private communication).

<sup>42</sup> S. Hochberg, H. S. W. Massey, H. Robertson, and L. H. Underhill, Proc. Phys. Soc. (London) **A68**, 746 (1955).

It is interesting to note that because the  $\text{He}^3(n,p)\text{T}$  reaction cross section is known to approach a  $1/v$  dependence at low energies, the elastic cross section should approach a constant.<sup>43</sup> From the known values of  $\sigma_T$  down to  $E_n = 0.14$  Mev, and the reaction cross sections  $\sigma_{ne}$  obtained from the inverse reaction by reciprocity,<sup>35</sup> it may be calculated that  $\sigma_e = \sigma_T - \sigma_{ne}$  is *already* substantially constant at a value of about 2 barns between 0.14 and 1 Mev, and may accordingly be expected to have that same value for all lower energies.

The present work fills the experimental gap in the neutron branch of the data for the system of four nucleons so that a conjoint analysis of all relevant data can be made.<sup>6</sup> The four-nucleon problem is also being investigated from the point-of-view of two-body forces, in the light of the effective-interaction theory of Brueckner.<sup>44</sup> Comparison of these neutron data with the analogous proton data is difficult at low energies because of the complication of Coulomb scattering, but the backscattering of corresponding cases is quite similar, particularly for  $n$ - $\text{He}^3$  and  $p$ -T. The 6-Mev  $n$ - $\text{He}^3$  data are in very close absolute agreement with recent measurements of  $p$ -T scattering at  $E_p = 6.5$  Mev over the common angular range between 20° and 160°; a graph showing this comparison has been published.<sup>45</sup>

It may be seen in Fig. 5 that the most significant difference between the  $n$ -T and  $n$ - $\text{He}^3$  cases appears in the  $B_1$  Legendre coefficient, and this might also be expected in the  $p$ -T and  $p$ - $\text{He}^3$  cases. In examining the whole set of nucleon: mass-three scattering data now

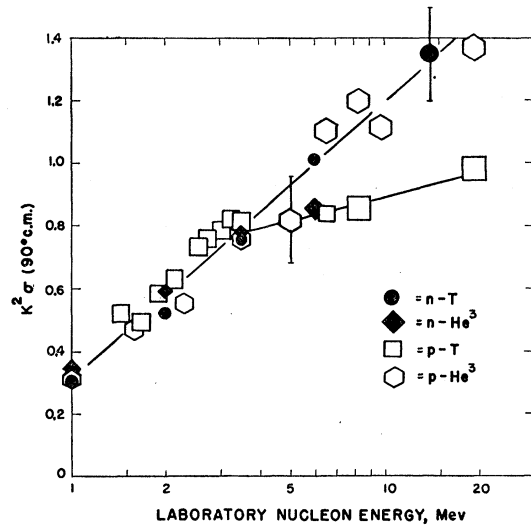


FIG. 7. Values of  $k^2\sigma(90^\circ \text{ c.m.})$  for all available data for nucleon scattering by tritium and  $\text{He}^3$ , plotted as a function of neutron energy. Above an energy of about 4 Mev, the  $n$ - $\text{He}^3$  and  $p$ -T data lie on a different branch from the  $n$ -T and  $p$ - $\text{He}^3$  data.

<sup>43</sup> See, for example, the discussion on pp. 438 and 439 of the textbook by L. D. Landau and E. M. Lifshitz, *Quantum Mechanics: Non-Relativistic Theory* (Addison-Wesley Publishing Company, Inc., Reading, Massachusetts).

<sup>44</sup> J. E. Young, Los Alamos Scientific Laboratory (private communication).

<sup>45</sup> See Fig. 6 of reference 9.

available for systematic regularities and trends, it was noticed that at energies above 5 Mev the  $p$ -T and  $n$ -He<sup>3</sup> data showed minima near 120° with a much smaller cross section than in the corresponding  $p$ -He<sup>3</sup> and  $n$ -T data. A marked difference was also observed in the 90° cross sections with greater consistency, due in part to the greater precision with which that cross section can be determined by least-squares fitting, and in part to the fact that the odd-numbered Legendre polynomials vanish at that angle. The striking effect which appears is presented in Fig. 7, where  $k^2\sigma(90^\circ)$  is plotted against the nucleon energy on a logarithmic scale for all available absolute cross section measurements of nucleon scattering by nuclei of mass three—some 30 different cases.<sup>46</sup> The data fall into two distinct classes above a nucleon energy of about 4 Mev. The logarithmic scale was used as a matter of convenience and because the data then seemed to fall on straight lines. It has been suggested that this is an effect of the threshold for the reaction of disintegration into two deuterons,<sup>47</sup> in which case it may be possible to derive useful infor-

<sup>46</sup> Since Fig. 7 was prepared, further measurements of  $p$ -He<sup>3</sup> scattering at five energies between 5.5 and 9.6 Mev have been reported by K. P. Artemov, S. P. Kalinin, and L. N. Samoilov, in *Zhur. Eksp. i Teoret. Fiz.* **37**, 663 (1959) [translation: *Soviet Phys.-JETP* **10**, 403 (1960)]. Neither numerical values nor absolute errors are given, but the data points plotted appear to be about 20% lower than corresponding points of the absolute measurements at neighboring energies in references 9 and 13. If the new data are uniformly raised 20%, then all five values of  $k^2\sigma(90^\circ)$  fall close to the upper line in Fig. 7.

<sup>47</sup> I. A. Baz' (private communication).

mation about the phase shifts and mixing parameters in the four-nucleon system.<sup>6</sup> Alternatively, it may constitute evidence for an extremely broad state of He<sup>4</sup> which first appears at an excitation of about 25 Mev, interfering with a state homologous to states of H<sup>4</sup> and Li<sup>4</sup>.<sup>44</sup>

In conclusion, gratification over the success of the calculations of Bransden, Robertson, and Swan must be tempered with the recognition that the Serber force is an oversimplified internucleon potential. A satisfactory interpretation of the observed agreement must await more refined calculations based on more realistic nuclear interactions.

#### ACKNOWLEDGMENTS

The authors are pleased to acknowledge the assistance of Dana L. Douglass in operating the accelerator and in the compilation of our data. We are indebted to C. J. Everett for the Monte Carlo calculations, and to A. C. Briesmeister, R. H. Sherman, and F. Edeskuty for assistance in the design and preparation of the samples. We wish to thank J. E. Young for his interest in and discussion of the results, and B. H. Bransden for his helpful correspondence and additional calculations during the course of our work. We are grateful to C. S. Wu for the opportunity to see the Columbia results for  $n$ -He<sup>3</sup> elastic and nonelastic cross sections<sup>48</sup> in advance of publication.

<sup>48</sup> A. Sayres, K. W. Jones, and C. S. Wu, *Bull. Am. Phys. Soc.* **3**, 365 (1958).